Quaternized chitosan as support for the assembly of gold nanoparticles and glucose oxidase: Physicochemical characterization of the platform and evaluation of its biocatalytic activity

Maria V. Bracamonte[a], Soledad Bollo[b], Pierre Labbé[c], Gustavo A. Rivas[a], Nancy F. Ferreyra[a,*]

[a] INFIQC, Departamento de Fisicoquímica, Facultad de Ciencias Químicas, Universidad Nacional de Córdoba, Haya de la Torre s/n, 5000 Córdoba, Argentina
[b] Laboratorio de Bioelectroquímica, Facultad de Ciencias Químicas y Farmacéuticas, Universidad de Chile, P.O. Box 233, Santiago, Chile
[c] Departement de Chimie Moléculaire, Université Joseph Fourier, UMR CNRS 5250, 38041 Grenoble Cedex 9, France

ARTICLE INFO

ABSTRACT

We report for the first time the use of quaternized chitosan (QCHI) for the immobilization of gold nanoparticles (NP) and glucose oxidase (GOD), the characterization of the resulting platform and its biocatalytic activity using glucose as substrate. The chemical substitution of chitosan has allowed us to work at physiologic pH to build up self-assembled layers of QCHI-NP as platform for the enzyme immobilization. The adsorption of GOD was analyzed by surface plasmon resonance (SPR) to compare the surface coverage of GOD in absence and presence of the QCHI-NP platform. The results obtained with cyclic voltammetry and scanning electrochemical microscopy (SECM) revealed that the adsorption of NP improves the conductivity of the structure and its electrochemical reactivity, facilitating the oxidation of the hydrogen peroxide produced by GOD. The electrodes modified with NP present higher amperometric response demonstrating the efficient transduction of the enzymatic activity in this structure.

1. Introduction

Gold nanoparticles (NP) have demonstrated to provide a suitable microenvironment for the immobilization of biomolecules. The characteristics of gold nanoparticles such as high surface-to-volume ratio, high surface energy, and their efficiency as electron-conducting pathways have been the reasons to facilitate the electron transfer between redox proteins and electrode surfaces [1–3]. These properties have led to an intensive use of this nanomaterial for the construction of electrochemical biosensors with improved analytical performance compared to other designs of biosensors [4,5].

Different methodologies have been used to build up structures combining NP and biomolecules. Among them, the layer-by-layer (LbL) technique, based on the electrostatic interaction of polyelectrolytes of opposite charge, have demonstrated to be highly successful. It allows the rational design of multilayered nanostructures in a reproducible way and the efficient immobilization of biomolecules [6]. The selection of the polymer to connect NP and biomolecules is crucial for the analytical performance of the resulting architecture. The natural polycation chitosan (CHI) is a copolymer of 1–4 linked of N-acetyl-β-glucosamine and β-glucosamine units. The biocompatibility, biodegradability, and bioactivity of CHI associated with desirable physical and mechanical properties have made this polymer an interesting element to develop biosensors [7,8].

CHI and gold nanoparticles have been employed in different designs of electrodes to develop (bio)sensors. In this sense, electrochemical deposition has been recently reported to prepare a chitosan–gold nanoparticles nanocomposite for the construction of non-enzymatic [9] and enzymatic glucose sensors [10–13]. A biosensor based on LbL assembly of CHI, NP and GOD at Pt electrode has been reported [14]. GOD was also immobilized in self-assembled structures with CHI and the film was used to reduce a gold salt to yield metallic gold nanoparticles [15].

Despite of the successful use of natural CHI in the design of biosensors, the polymer present the inconvenience of its low solubility at physiological pH [16]. In order to improve CHI solubility, we substituted a percentage of CHI amine functions by methyl groups to obtain quaternized amines. This chemical modification gives place to a polymer, named quaternized chitosan (QCHI), with permanent positive charge at any pH and soluble even in phosphate buffer [17].

We report for the first time, the use of QCHI for the immobilization of NP and GOD, the characterization of the resulting platform and its biocatalytic activity using glucose as substrate The procedure for the preparation of the electrodes involves two steps:

* Corresponding author. Tel.: +54 351 4334169; fax: +54 351 4334188.
E-mail addresses: ferreyra@fcq.unc.edu.ar,
nancy_ferreyra@yahoo.com (N.F. Ferreyra).

first, the LBL self-assembly of QCHI and NP at thiolated gold electrodes as electrochemical platform; and second, the adsorption of QCHI-GOD multilayers on this platform as biosensing element. We present the electrochemical characterization of the QCHI-NP platform, the analysis of GOD adsorption at the QCHI-NP electrode by surface plasmon resonance (SPR), as well as the analysis of the bioelectrocatalytic activity of the immobilized GOD by scanning electrochemical microscopy (SECM) and amperometry.

2. Experimental

2.1. Reagents

Gold nanoparticles (NP) citrate stabilized of 10 nm nominal diameter (Catalog number G-1527) and glucose oxidase (GOD) (Type X-S, Aspergillus niger, EC 1.1.3.4, 210,000 Units per gram of solid, MW 160 kDa), were obtained from Sigma. Hydrogen peroxide (30% V/V aqueous solution) was from Baker. Ferrocenemethanol (FcOH) and 3-mercapto-1-propanesulfonic acid (MPS) were from Aldrich. Chitosan (Pronova, Norway) with molecular weight of 190,000 g mol^{-1} was used for preparing the quaternized chitosan (QCHI) as described in reference [17]. The average molecular weight of the resulting QCHI was 52,750 g mol^{-1} and the content of quaternized amine 40.0 mol%. Other chemicals were reagent grade and used without further purification. All solutions were prepared with ultra-pure water (18 MΩ cm) from a Millipore MilliQ system.

2.2. Equipment

Cyclic voltammetry (CV) and amperometry were performed with an EPSILON potentiostat (Bioanalytical Systems Inc., USA). Scanning Electrochemical Microscopy was performed with a CHI 900 (CH Instruments Inc., USA). A ca. 10 μm diameter homemade carbon fiber electrode served as ultramicroelectrode (UME), while gold disk electrodes (Au) of 3 mm diameter (CHI 101) were used as substrate. A rotating disk electrode (RDE) of gold (2 mm of diameter, Radiometer Analytical, model EDI101 with tip model 35T110) was used in connection with a speed control unit (Radiometer Analytical, Model CTV101). In all the experiments a platinum wire and Ag/AgCl, 3 M NaCl (BAS, Model RE-5B) were used as counter and reference electrodes, respectively. The experiments were performed at room temperature.

SPR measurements were done with a single channel, AUTOLAB SPRINGLE instrument (Eco Chemie, The Netherlands). The SPR sensor disks (BK 7) were mounted on a hemicylindrical lens through index-matching oil to form the base of a cuvette. Sample solutions (60 μL) were injected manually into the cuvette. The measurements were carried out under non-flow liquid conditions at 25 °C.

2.3. Modification of gold surfaces

The cleaning procedure of gold electrodes included polishing with 0.05 μm alumina for 6 min, careful sonication in deionized water for 5 min, and immersion in "Piranha" solution (1:3 v/v H$_2$O$_2$/98% H$_2$SO$_4$) for 5 min, followed by a rinsing step with ultrapure water. *Caution: "Piranha" solution is very corrosive and must be handled with care.* The clean surfaces were stabilized by cycling the potential between 0.200 V and 1.650 V at 10 V s^{-1} in 0.50 mol dm^{-3} sulfuric acid solution until obtaining a reproducible response. Before each experiment, the surface was checked by CV at 0.100 V s^{-1} in fresh 0.50 mol dm^{-3} sulfuric acid solution.

The adsorption of MPS was performed by soaking the electrode for 30 min in a 2.00 × 10^{-2} mol dm^{-3} MPS solution prepared in 1.6 × 10^{-3} mol dm^{-3} sulfuric acid solution, followed by a careful rinsing with deionized water.

Construction of QCHI-NP platform: The multilayer was obtained by alternating immersion of the electrode in QCHI and NP solutions. QCHI adsorption was performed by immersion in a 0.50 mg mL^{-1} QCHI solution prepared in 5.00 × 10^{-2} mol dm^{-3} phosphate buffer pH 7.40 for 20 min. NP were adsorbed for 60 min from the commercial solution. After each adsorption step, the surfaces were copiously rinsed with 5.00 × 10^{-2} mol dm^{-3} phosphate buffer pH 7.40. The resulting electrodes are indicated as Au/MPS/(QCHI-NP)$_n$, being n the number of QCHI-NP adsorption steps. The effect of NP adsorption time was evaluated by varying the immersion time of Au/MPS/QCHI electrodes in the NP solution between 15 and 120 min.

Construction of QCHI-GOD multilayer: The adsorption of the enzyme was carried out by alternating immersion of Au/MPS electrodes in 0.50 mg mL^{-1} QCHI solution for 20 min and 1.0 mg mL^{-1} GOD solution for 30 min. Both solutions were prepared in 5.00 × 10^{-2} mol dm^{-3} phosphate buffer pH 7.40. After each adsorption step, the electrodes were copiously rinsed with the phosphate buffer solution. The resulting electrodes are indicated as Au/MPS/(QCHI-GOD)$_m$, being m the number of QCHI-GOD adsorption steps.

The same procedures were done for electrodes previously modified with the QCHI-NP platform, being indicated as Au/MPS/(QCHI-NP)$_n$/(QCHI-GOD)$_m$.
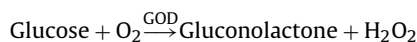
2.4. Measuring procedures
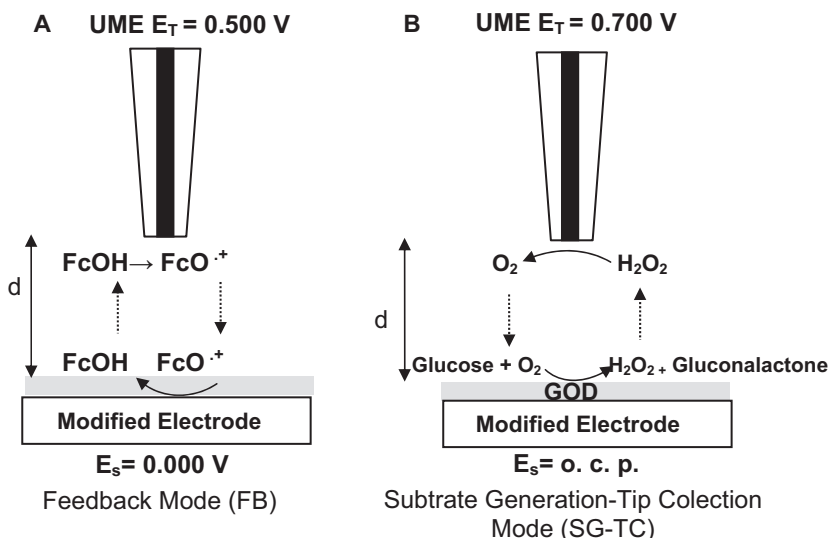
2.4.1. SECM

Is a powerful tool that makes possible to obtain information about chemical reactivity at interfaces, and kinetic data of heterogeneous reactions [18]. It is a scanning probe technique that uses a positionable UME as probe [19]. We employed SECM to evaluate the electrochemical reactivity of the modified electrodes using feedback mode (FB), Scheme 1A. This method is based on the measurement of the current produced at the UME, i_T, when it is brought close to the substrate in the presence of a redox mediator [20,21]. The steady-state current of the UME positioned far from the substrate is $i_{T,\infty} = 4naFDC$. In diffusion-controlled positive feedback case, $i_T > i_{T,\infty}$, the substrate acts as a conductive surface producing an additional flux of the redox mediator at the UME. On the contrary, in the negative feedback case, $i_T < i_{T,\infty}$, the substrate acts as an electrical insulator and hinders the flux of the redox mediator at the UME surface [22].

In our experiments, FcOH (5.0 × 10^{-4} mol dm^{-3} solution) was used as redox mediator. The UME and the substrate potentials were held at 0.500 V and 0.000 V, respectively, to allow the feedback takes place between both electrodes (see Scheme 1A). A series of constant high images of the modified electrodes was obtained following the procedure described in [3]. The results are presented in a dimensionless form normalizing the experimental feedback current, i_T, by the steady-state current $i_{T,\infty}$.

SECM was also used to detect the enzymatic activity of the immobilized GOD. The analysis was performed in substrate generation-tip collection mode (SG-TC) (Scheme 1B). In this operation method, the UME is approached to the surface modified with the enzyme. In the presence of the substrate the reaction takes place and the enzymatic activity is monitored at the UME by applying a potential appropriated to detect an electroactive product of the enzymatic reaction [23]. In our experiments, the detection of GOD activity was based on the measurement of the hydrogen peroxide formed according to the following reaction (see Scheme 1B):

$$\text{Glucose} + \text{O}_2 \xrightarrow{\text{GOD}} \text{Gluconolactone} + \text{H}_2\text{O}_2$$

The UME was first positioned using FcOH, as described in reference [3]. The surface was carefully washed and the cell filled with

Scheme 1. SECM experimental setup employed for (A) Feedback and (B) SG-TC mode. E_T and E_s, correspond to UME and substrate applied potential, respectively, and d is the distance between the UME and the substrate.

5.00×10^{-2} mol dm^{-3} phosphate buffer solution pH 7.40. The UME was then polarized at 0.700 V and an image of 250 μm × 250 μm was recorded at 20 μm s^{-1} to obtain the background current. After returning the UME to the starting position ($x = 0$, $y = 0$), the buffer solution was replaced by a 5.00×10^{-2} mol dm^{-3} glucose solution and a new scan was performed. When GOD is active, the hydrogen peroxide produced by the enzymatic reaction at the electrode is oxidized on the UME at the applied potential producing an increase in the current.

2.4.2. Surface plasmon resonance (SPR)

This technique makes possible to monitor *in situ* interfacial processes such as adsorption/desorption of molecules with molecular weight higher than 1 kDa [24–27]. In this work, SPR experiments were carried out to evaluate the adsorption of GOD at Au/MPS/(QCHI-NP)$_n$ or at Au/MPS electrodes. Gold disks where modified with MPS, rinsed with deionized water and inserted into the SPR cell. An aliquot of 60 μL of 5.00×10^{-2} mol dm^{-3} phosphate buffer pH 7.40 was added to the cell to obtain a baseline signal. The buffer was drained using a peristaltic pump and replaced by 60 μL of 0.50 mg mL^{-1} QCHI solution. The interaction was monitored until obtaining a constant value of SPR angle. The system was then washed several times with buffer solution and 60 μL of phosphate buffer where placed in the cell to record a new baseline. The adsorption of GOD was performed in a similar way by using 60 μL of 1.0 mg mL^{-1} GOD solution. The variation of SPR angle, $\Delta\theta$, was determined as the difference between the corresponding base lines values before and after the adsorption step. Similar experiments were performed to determine the amount of GOD adsorbed at Au/MPS/(QCHI-NP)$_n$/(QCHI-GOD)$_m$ electrodes.

2.4.3. Amperometric experiments

Amperometric experiments were carried out by applying the desired potential, allowing the transient current to decay prior to the addition of the analyte and monitoring the subsequent current.

3. Results and discussion

3.1. Electrochemical characterization of Au/MPS/(QCHI-NP)$_1$ platform

3.1.1. Analysis by SECM, CV and RDE

Gold electrodes modified by self-assembling of MPS, QCHI, and NP were characterized by SECM using FB mode. Fig. 1 dis-

plays images obtained at bare gold (a), Au/MPS/QCHI (b) and Au/MPS/(QCHI-NP)$_1$ with NP adsorption times of 60 (c) and (d) 120 min. The image of the bare electrode, presents a typical substrate conductive behavior, with homogeneous current values of 1.25 times $i_{T,\infty}$ [22]. After QCHI adsorption, the normalized current decreases to 1.12 $i_{T,\infty}$ as average. This behavior is compatible with a negative feedback between the UME and the substrate, indicating that QCHI partially blocks the electrochemical response of FcOH. This effect is associated with the electrostatic repulsion between FcO$^{\cdot+}$ formed at the UME and the positive charges of QCHI at the modified surface. Similar behavior has been previously reported for the adsorption of CHI at glassy carbon electrodes [28]. When NP are adsorbed, the normalized current increases to 1.19 $i_{T,\infty}$ and 1.31 $i_{T,\infty}$, for 60 and 120 min, respectively. In the last case, the normalized current is higher than $i_{T,\infty}$ of the bare electrode (note that in Fig. 1d the current color scale is different). This electrochemical behavior can be associated with an increase in the electroactive area of the surface or with a higher charge transference constant of the redox compound at the modified surface. To evaluate this aspect, we analyzed the electrochemical response of FcOH by CV and RDE.

Fig. 2 presents the cyclic voltammograms obtained at 0.100 V s^{-1} in 5.0×10^{-4} mol dm^{-3} FcOH (prepared in NaClO$_4$ 0.500 mol dm^{-3}) at bare gold electrode (a), and at gold electrodes after adsorption of MPS (b), QCHI (c), and NP for 60 (d), and 120 (e) min. As expected, for FcOH, the voltammogram at bare gold electrode indicates a diffusion controlled oxidation process with peak potential separation (ΔE_p) of 64 mV and anodic peak current (I_{pa}) of 2.8 μA, in agreement with previous reports [3,29]. Upon modification with MPS and QCHI, the voltammograms exhibit a decrease in peak currents of 4% and 22% and a substantial increase of ΔE_p up to 87 and 123 mV, respectively. These results indicate that MPS and QCHI behave as a barrier for the electrochemical process. Accordingly, the kinetics of FcOH oxidation process is determined by the rate of the electron transfer across the film [29]. After NP adsorption, there is a diminution of ΔE_p and enhancement of I_{pa}. The corresponding values for ΔE_p and I_{pa} are 67 and 60 mV and 3.15 and 3.20 μA for, 60 and 120 min of adsorption, respectively. These effects indicate a faster electron transfer kinetics due to the presence of NP. Similar results were also obtained using [Fe(CN)$_6$]$^{3-}$ and [Fe(CN)$_6$]$^{4-}$ as redox probes (not shown), in agreement with previous reports [30,31].
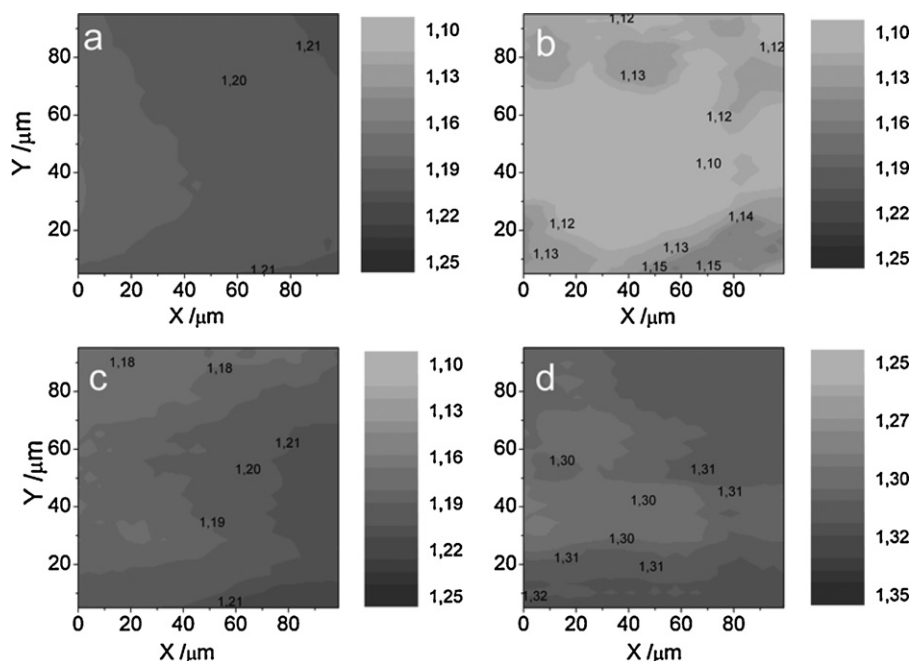
Fig. 1. Surface-plot images of (a) Au, (b) Au/MPS/QCHI, and Au/MPS/(QCHI-NP)$_1$ with (c) 60 and (e) 120 min of NP adsorption time. Numbers on the images correspond to normalized current values. Experimental conditions: 5.0×10^{-4} mol dm^{-3} FcOH, supporting electrolyte: 0.050 mol dm^{-3} phosphate buffer pH 7.40, $E_T = 0.500$ V and $E_s = 0.000$ V vs. (Ag/AgCl/3 M NaCl)/V and 10 μm s^{-1} UME scan rate. The results are presented in a dimensionless form normalizing the experimental feedback current, i_T, by the steady-state current $i_{T,\infty}$.

To evaluate the effect of NP in the electron transfer process, we determine the charge transfer constant, k^0, of FcOH by RDE. The values obtained from Tafel plots are: 7.0×10^{-3} cm s^{-1} for bare gold, and 8.3×10^{-4}; 2.8×10^{-2}, and 2.9×10^{-2} cm s^{-1} for Au/MPS/(QCHI-NP)$_1$ with 15, 30, and 120 min of NP adsorption, respectively. These values clearly show a significant improvement of the electron transfer process as the NP surface coverage increases.

3.1.2. Electrochemical response to hydrogen peroxide

Since the reaction used to detect the activity of GOD incorporated in the multilayer system is based on the electrochemical response of hydrogen peroxide, we evaluate the effect of NP on the electrochemical reaction of this compound by CV at Au/MPS/QCHI and Au/MPS/(QCHI-NP)$_1$ with increasing NP adsorption time (Fig. 3). The electrochemical response of hydrogen peroxide is completely blocked at Au/MPS/QCHI electrode (a), while the oxidation current at 0.700 V, are 66.2, 85.1, 139.8, and 142.0 μA for 30, 90, 120, and 150 min of NP adsorption time, respectively. The adsorption of NP clearly enhances the hydrogen peroxide electrochemical response, being this effect more important for the oxidation than for the reduction process. No additional increase in the currents was observed after 120 min of NP adsorption, in agreement with our results observed for FcOH and ferrocyanide.
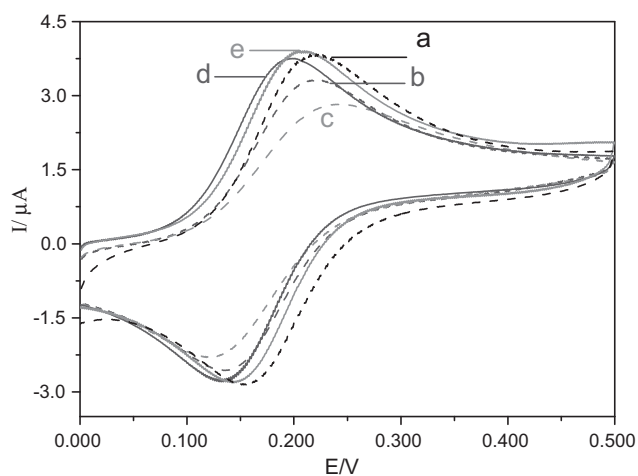

Fig. 2. Cyclic voltammograms obtained at 0.100 V s^{-1} on: (a) Au (---), (b) Au/MPS (▬ ▬ ▬), (c) Au/MPS/QCHI (▬ ▬ ▬), and Au/MPS/(QCHI-NP) with (d) 60 (—), (e) 120 min (▬▬) of NP adsorption time. Experimental conditions: 5.0×10^{-4} mol dm^{-3} FcOH solution. Supporting electrolyte 0.500 mol dm^{-3} NaClO$_4$. Potential vs. (Ag/AgCl/3 M NaCl)/V.
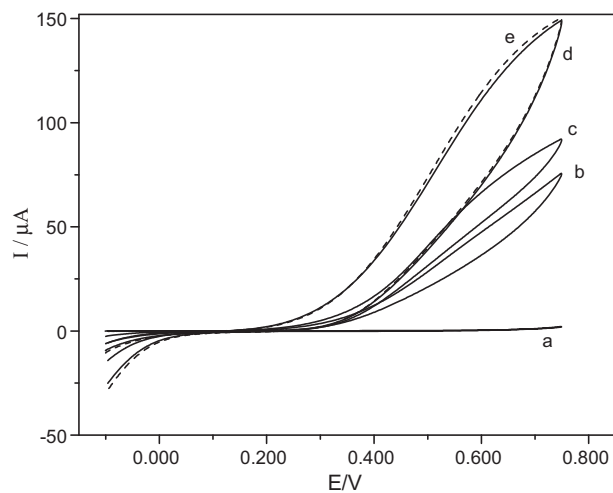

Fig. 3. Cyclic voltammograms obtained at 0.100 V s^{-1} on (a) Au/MPS/QCHI and Au/MPS/(QCHI-NP)$_1$ electrodes with (b) 30, (c) 90, (d) 120 and (e) 150 min of NP adsorption time. Experimental conditions: 1.00×10^{-2} mol dm^{-3} H$_2$O$_2$ solution, supporting electrolyte 0.050 mol dm^{-3} phosphate buffer pH 7.40. Potential vs. (Ag/AgCl/3 M NaCl)/V.
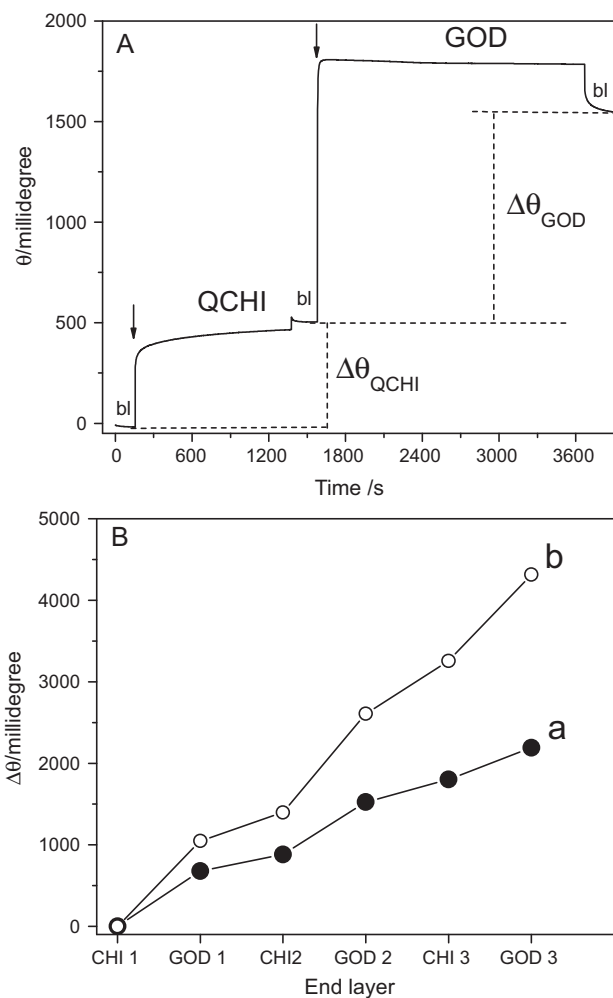
Fig. 5. Surface-plot images obtained in SG-TC mode at Au/MPS/(QCHI-GOD)$_1$, (plot a and c), and Au/MPS/(QCHI-NP)$_1$/(QCHI-GOD)$_1$ (plot b and d), electrodes. Images c and d were obtained in 0.050 mol dm^{-3} glucose solution while images a and b were acquired in phosphate buffer pH 7.40. Experimental conditions: $E_T = 0.700$ V vs. (Ag/AgCl/3 M NaCl) and E_s at o.c.p. Image parameters: 250 μm × 250 μm, 20 μm s^{-1} UME scan rate.

layer. Form these values; it is possible to obtain the amount of GOD adsorbed on both surfaces [27]. Table 1 presents $\Delta\theta$ and the surface coverage of GOD (Γ_{GOD}) for the adsorption of 1, 2 and 3 bilayers of (QCHI-GOD) at Au/MPS and Au/MPS/(QCHI-NP)$_1$ platforms. To calculate Γ_{GOD} we consider that 120 millidegree of SPR angle displacement corresponds to 1 ng mm^{-2} of adsorbed protein [27]. Average values of 4.3×10^{12} and 2.1×10^{12} molecules cm^{-2} for each GOD adsorption step were obtained at Au/MPS and Au/MPS/(QCHI-NP)$_1$, respectively. The lower $\Delta\theta$ and Γ_{GOD} values obtained in the presence of NP indicate that QCHI-NP layer is less efficient for the following QCHI and GOD adsorption. Therefore, a larger amount of enzyme is adsorbed in the absence of nanoparticles.

3.3. Evaluation of GOD enzymatic response

3.3.1. SECM in SG-TC mode

SECM experiments in SG-TC mode were carried out to evaluate GOD activity at the modified surfaces. Fig. 5 displays SECM images of Au/MPS/(QCHI-GOD)$_1$ (plots a and c), and Au/MPS/(QCHI-NP)$_1$/(QCHI-GOD)$_1$ (plots b and d) platforms. In the last case the selected NP adsorption time of NP was 60 min. The activity of the enzyme confined to the electrode surface can be clearly observed from the corresponding difference between the current values before (a and b) and after (c and d) the addition of glucose. Average background currents of 2 and 5 pA are detected, while after the addition of glucose an increase up to 15 pA and 30 pA is observed for Au/MPS/(QCHI-GOD)$_1$ and Au/MPS/(QCHI-NP)$_1$/(QCHI-GOD)$_1$, respectively. The adsorption of one bilayer of QCHI-NP as platform for the enzyme adsorption makes possible to obtain a higher enzymatic response. These results are associated to a higher electrochemical reactivity of the surface due to the presence of NP,

Fig. 4. (A) Sensorgrams for QCHI and GOD adsorption at Au/MPS. The arrows indicate the injection of QCHI or GOD after recording the base line in buffer solution. (B) $\Delta\theta$ values for the adsorption of GOD at Au/MPS/(QCHI-NP) (a), and Au/MPS (b) platforms.

3.2. Evaluation of GOD adsorption by SPR

We evaluate the amount of GOD immobilized at two platforms: Au/MPS and Au/MPS/(QCHI-NP)$_1$. Fig. 4A displays the sensorgram for the adsorption of QCHI and GOD at Au/MPS. As it was previously indicated, the baseline was obtained in 0.050 mol dm^{-3} phosphate buffer solution pH 7.40. After the injection of QCHI, there is an increase in the resonance angle shift, $\Delta\theta$. After washing the surface with phosphate buffer to remove the weakly bound QCHI, the solution of GOD is injected and a new increase in the resonance angle due to the enzyme immobilization is observed. The procedure is repeated to obtain the structure with the desired number of bilayers. Fig. 4B presents $\Delta\theta$ values for successive adsorption of GOD and QCHI on Au/MPS/(QCHI-NP)$_1$ (a), and Au/MPS (b) platforms. For comparison, $\Delta\theta$ are normalized by the value of QCHI
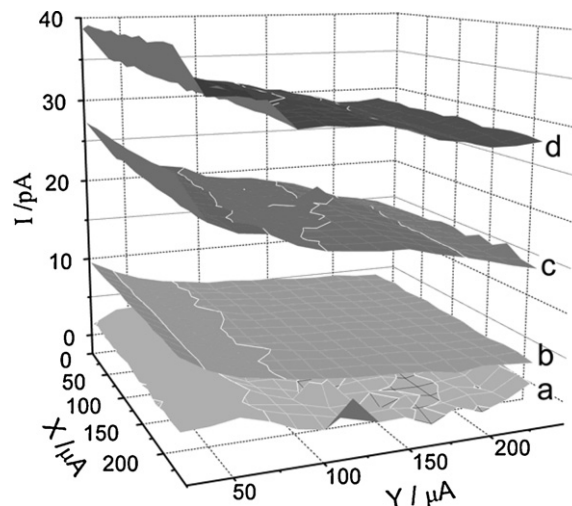
Table 1
Shift of SPR angle ($\Delta\theta$) and surface coverage (Γ_{GOD}) for GOD adsorption as a function of the number of QCHI-GOD bilayers[a].

m	Au/MPS/(QCHI-GOD)$_m$		Au/MPS/(QCHI-NP)$_1$/(QCHI-GOD)$_m$	
	$\Delta\theta/10^2$ millidegree	$\Gamma_{GOD}/10^{12}$ molecule cm^{-2}	$\Delta\theta/10^2$ millidegree	$\Gamma_{GOD}/10^{12}$ molecule cm^{-2}
1	(12 ± 3)	3.8	(6.85 ± 0.09)	2.1
2	(15 ± 3)	4.7	(7 ± 1)	2.2
3	(14 ± 5)	4.4	(6 ± 2)	1.9

[a] The values correspond to the average of three independent experiments.

Table 2
Analytical parameters for Au/MPS/(QCHI-NP)$_n$/(QCHI-GOD)$_m$ electrodes in the presence of glucose.

Structure		(Sensitivity/10^1) μA M^{-1}	(LOQ/10^{-3}) mol dm^{-3}	(Linear range/10^{-3}) mol dm^{-3}	Time of responses
n	m				
0	1	(4 ± 1)	1.77	0.5–1.5	4.0
	2	(16 ± 3)	0.42	0.1–1.5	4.5
	3	(23 ± 3)	0.20	0.06–2.15	5.0
1	1	(9 ± 1)	0.88	0.3–1.3	5.0
	2	(25 ± 2)	0.24	0.07–1.6	4.5
	3	(29 ± 5)	0.09	0.03–1.0	4.5
2	1	(18 ± 2)	0.39	0.12–1.1	2.0
	2	(31 ± 3)	0.16	0.08–2.0	3.0
	3	(26 ± 2)	0.22	0.07–1.6	2.3
3	1	(19 ± 5)	0.39	0.1–1.0	2.0

Multilayers were built on the top of Au/MPS electrode. Each value is the average of five independent experiments.

since SPR experiment showed that the amount of GOD adsorbed on Au/MPS/(QCHI-NP)$_1$ is lower than on Au/MPS/QCHI. Experiments made in different regions of the same surface showed small variation between current values, indicating a homogeneous distribution of the enzyme on the modified electrode.

3.3.2. Electrochemical response to glucose

The effect of the amount of NP on the enzymatic response of GOD was also evaluated from calibration curves obtained from amperometric experiments performed at 0.700 V for successive additions of glucose. The sensitivities achieved at Au/MPS/(QCHI-NP)$_1$/(QCHI-GOD)$_1$ electrodes as function of NP adsorption time were $(4 ± 1) × 10^1$ μA mol^{-1} dm^3, $(4 ± 1) × 10^1$ μA mol^{-1} dm^3, $(9 ± 1) × 10^1$ μA mol^{-1} dm^3, $(1.5 ± 0.2) × 10^2$ μA mol^{-1} dm^3, and $(1.5 ± 0.3) × 10^2$ μA mol^{-1} dm^3 for 0, 30, 60, 90 and 120 min, respectively. An enhancement in the sensitivity to glucose is observed with the increase in adsorption time of NP up to 90 min, in agreement with the increase of NP surface coverage described above.

To determine the biocatalytic activity of the enzyme incorporated in the structure we evaluate the response of different platform, Table 2 summarizes the analytical parameters of bioelectrodes with different architectures. As the number of QCHI-GOD bilayers increases, an augment of sensitivity and a decrease in LOQ is observed. The comparison between the results obtained with Au/MPS/(QCHI-NP)$_n$/(QCHI-GOD)$_m$ electrodes with equivalent number of QCHI-GOD bilayers (m) for 0, 1, 2 or 3 bilayers of QCHI-NP shows that, in the presence of NP, there are an increase of sensitivity, and a decrease of LOQ and time of response. The most significant effect is obtained with two bilayers of QCHI-NP,

as it is shown in Fig. 6A, that corresponds to the amperometric recordings at 0.700 V for Au/MPS/(QCHI-GOD)$_2$ (gray line), and Au/MPS/(QCHI-NP)$_2$/(QCHI-GOD)$_2$ (black line), for successive additions of $0.20 × 10^{-3}$ mol dm^{-3} of glucose and Fig. 6B that displays their corresponding calibration plots. It is evident that the presence of NP improves the response of the bioelectrode towards glucose.

Compared to other bioelectrodes based on the electrochemical deposition of NP on CHI, the sensitivity obtained with our more efficient platform was superior to that reported in [10] and similar to that obtained in [11], while the response times (time required to reach the 95% steady state response) were shorter than the informed in those references.

Compared to other bioelectrodes based on self-assembled multilayers containing NP, the response highly depends on the polyelecrolyte. In the case of natural CHI, self-assembled structures of six bilayers of CHI/GOD/NP at a Pt electrode modified with polyacrilic acid gave a sensitivity of 555 μA M^{-1}, that correspond to 92.5 μA M^{-1} per bilayer [14], similar to the value we obtain at Au/(QCHI-NP)$_1$/(QCHI-GOD)$_1$, but less than the value we determined with Au/(QCHI-NP)$_2$/(QCHI-GOD)$_1$. On the other hand, despite of the amount of protein adsorbed on to the QCHI-NP platform is smaller, the values of sensitivity we obtained for the same number of QCHI-GOD are 2.25 and 1.55 higher that those reported in [17] for one and two bilayers, respectively.

Ascorbic acid (AA), uric acid (UA) and acetaminophen (AP) in biological sample could be easily oxidized at low over potential, and often interfere with the detection of glucose. Even when the main goal of this work was the physical chemical characterization of the bioelectrodes, in order to evaluate its potential analytical application we use the permselective polymer Nafion (NF) as anti-
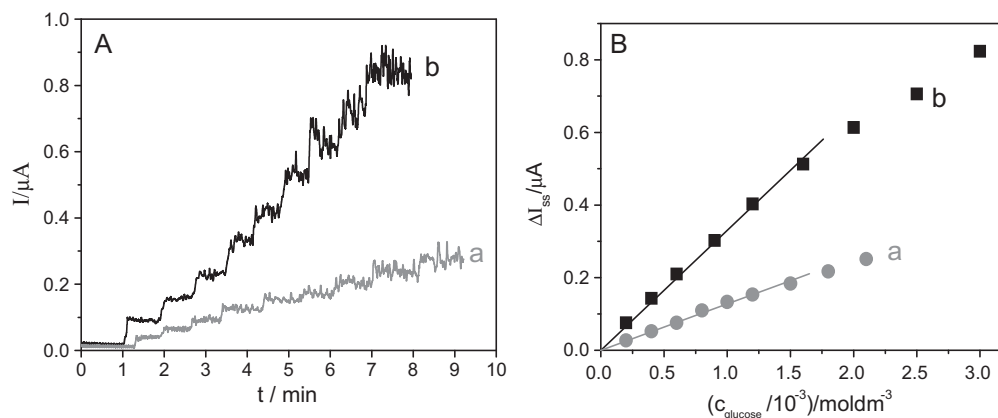

Fig. 6. (A) Amperometric response and (B) calibration plots for successive additions of $2.0 × 10^{-4}$ mol dm^{-3} at Au/MPS/(QCHI-GOD)$_2$ (a) and Au/MPS/(QCHI-NP)$_2$/(QCHI-GOD)$_2$ (b) electrodes. Experimental conditions: supporting electrolyte 0.050 mol dm^{-3} phosphate buffer solution pH 7.40 and working potential 0.700 V vs. (Ag/AgCl/3 M NaCl)/V.

interference layer. We adsorbed the polymer either as external layer or incorporated between QCHI-NP and QCHI-GOD bilayers. In the last case the interference of UA, AA and AP are largely decreased, although the selectivity is still non acceptable for glucose quantification in blood samples. Further work is necessary to do to evaluate and compare different alternatives to resolve this inconvenient.

4. Conclusions

It was demonstrated that gold electrodes modified with self-assembled multilayers of QCHI and NP represent a very interesting alternative for the immobilization of GOD. Voltammetric and SECM studies revealed a higher electrochemical reactivity of the structure due to the presence of NP with important improvement in the response of hydrogen peroxide at QCHI-NP platform. Surface plasmon resonance experiments demonstrated that $Au/MPS/(QCHI-NP)_n$ electrodes are less efficient than Au/MPS/QCHI for GOD adsorption. However, the presence of NP improves the conductivity of the structure, facilitating the oxidation of the hydrogen peroxide produced by GOD. As result of this effect, the electrodes modified with NP present higher amperometric response and better analytical performance, representing an important strategy for potential analytical applications.

Acknowledgements

References

[1] Sh. Guo, E. Wang, Anal. Chim. Acta 598 (2007) 181.
[2] Y.A. Zabet-Khosousi, Al-Amin Dhirani, Chem. Rev. 108 (2008) 4072.
[3] N.F. Ferreyra, S. Bollo, G.A. Rivas, J. Electroanal. Chem. 638 (2010) 262.
[4] E. Katz, in: S.Y. Yurish, M.T.S.R. Gomes (Eds.), Smart Sensors and MEMS, Kluwer Academic Publishers, Netherlands, 2005, Ch. 14.
[5] Sh. Guo, Sh. Dong, Trends Anal. Chem. 28 (2009) 96.
[6] J.R. Siqueira Jr., L. Caseli, F.N. Crespilho, V. Zucolotto, O.N. Oliveira Jr., Biosens. Bioelectron. 25 (2010) 1254.
[7] Luciano Caseli, S. David, dos Santos Jr., F. Ricardo, Aroca, N. Osvaldo, Oliveira Jr., Mater. Sci. Eng. C 29 (2009) 1687.
[8] D. Wei, Y. Ye, X. Jia, Ch. Yuan, W. Qian, Carbohyd. Res. 345 (2010) 74.
[9] D. Feng, F. Wang, Z. Chen, Sens. Actuators B 138 (2009) 539.
[10] X.L. Luo, J.J. Xu, Y. Du, H.Y. Chen, Anal. Biochem. 334 (2004) 284.
[11] Y. Du, X.L. Luo, J.J. Xu, H.Y. Chen, Bioelectrochemistry 70 (2007) 342.
[12] G.Q. Wu, Z.Y. Li, J. Clin. Rehabil. Tiss. Eng. Res. 13 (2009) 5789.
[13] X. Zenga, X. Li, L. Xing, X. Liu, Sh. Luo, W. Wei, B. Kong, Y. Li, Biosens. Bioelectron. 24 (2009) 2898.
[14] B.Y. Wu, S.H. Hou, F. Yin, J. Li, Z.X. Zhao, J.D. Huang, Q. Chen, Biosens. Bioelectron. 22 (2007) 838.
[15] L. Caseli, D.S. dos Santos Jr., M. Foschini, D. Gonçalves, O.N. Oliveira Jr., Mater. Sci. Eng. C 27 (2007) 1108.
[16] M.L. Tan, P.F.M. Choong, C.R. Dass, J. Pharm. Pharmacol. 61 (2009) 3.
[17] S.A. Miscoria, J. Desbrieres, G.D. Barrera, P. Labbé, G.A. Rivas, Anal. Chim. Acta 578 (2006) 137.
[18] M. Burchardt, G. Wittstock, Bioelectrochemistry 72 (2008) 66.
[19] X. Lu, Q. Wang, X. Liu, Anal. Chim. Acta 601 (2007) 10.
[20] J. Bard, F.F. Fan, J. Kwak, L. Ovadia, Anal. Chem. 61 (1989) 132.
[21] D.O. Wipf, A.J. Bard, J. Electrochem. Soc. 138 (1991) 469.
[22] S. Bollo, in: J.A. Squella, S. Bollo (Eds.), Electroanalytical Aspects of Biological Significant Compounds, Trandsworld Research Network, India, 2006, Ch. 6.
[23] M. Pellissier, D. Zigah, F. Barriére, Ph. Hapiot, Langmuir 24 (2008) 9089.
[24] X. Fan, I.M. White, S.I. Shopova, H. Zhu, J.D. Suter, Y. Sun, Anal. Chim. Acta 620 (2008) 8.
[25] J. Homola, Chem. Rev. 108 (2008) 462.
[26] R.K. Mendes, R.F. Carvalhal, L.T. Kubota, J. Electroanal. Chem. 612 (2008) 164.
[27] K.M. Aung, X. Ho, X. Su, Sens. Actuators B 131 (2008) 371.
[28] S. Bollo, N.F.G.A. Ferreyra, Rivas Electroanal. 19 (2007) 833.
[29] Ch. Mokrani, J. Fatisson, L. Guérente, P. Labbé, Langmuir 21 (2005) 4400.
[30] J.J. Kakkassery, J.P. Abid, M. Carrara, D.J. Fermín, Faraday Discuss. 125 (2004) 157.
[31] D. Du, J. Ding, J. Cai, A. Zhang, J. Electroanal. Chem. 605 (2007) 53.